EDGE ARTICLE

Check for updates

Reductive catalytic fractionation of pine wood: elucidating and quantifying the molecular structures in the lignin oil†

K. Van Aelst, [ID] E. Van Sinay, T. Vangeel, [ID] E. Cooreman, G. Van den Bossche, T. Renders, J. Van Aelst, S. Van den Bosch [ID] and B. F. Sels [ID] *

In-depth structural analysis of biorefined lignin is imperative to understand its physicochemical properties, essential for its efficient valorization to renewable materials and chemicals. Up to now, research on Reductive Catalytic Fractionation (RCF) of lignocellulose biomass, an emerging biorefinery technology, has strongly focused on the formation, separation and quantitative analysis of the abundant lignin-derived phenolic monomers. However, detailed structural information on the linkages in RCF lignin oligomers, constituting up to 50 wt% of RCF lignin, and their quantification, is currently lacking. This study discloses new detailed insights into the pine wood RCF lignin oil's molecular structure through the combination of fractionation and systematic analysis, resulting in the first assignment of the major RCF-derived structural units in the ^{1}H–^{13}C HSQC NMR spectrum of the RCF oligomers. Specifically, β-5 γ-OH, β-5 ethyl, β-1 γ-OH, β-1 ethyl, β-β 2x γ-OH, β-β THF, and 5-5 inter-unit linkages were assigned unambiguously, resulting in the quantification of over 80% of the lignin inter-unit linkages and end-units. Detailed inspection of the native lignin inter-unit linkages and their conversion reveals the occurring hydrogenolysis chemistry and the unambiguous proof of absence of lignin fragment condensation during proper RCF processing. Overall, the study offers an advanced analytical toolbox for future RCF lignin conversion and lignin structural analysis research, and valuable insights for lignin oil valorization purposes.

Introduction

Recent studies have shown that lignocellulosic biomass (*e.g.* wood, agricultural and forestry residues, and grasses) holds enormous potential for the sustainable production of chemicals and fuels.[1–7] Given its complex structure of intertwined cellulose, hemicellulose and lignin biopolymers, lignocellulose is fractionated in a biorefinery prior to further downstream processing of each intermediate fraction into marketable end products, such as sugar- or lignin-derived chemicals (*e.g.* phenol,[7,8] terephthalic acid[9] and 5-HMF[10]) or fuels (*e.g.* bioethanol,[11] light bionaptha[6,12]), paper, or other materials.[3,5,13–15]

One of the foremost biorefinery challenges is the simultaneous valorization of these three biopolymers, given the reactive nature of these biopolymers in various (*i.e. acidic* or *alkaline*) biorefinery conditions. Besides hemicellulose due to humification,[16,17] lignin is one of the most challenging lignocellulosic constituents.[2,5,18]

Centre for Sustainable Catalysis and Engineering, KU Leuven, Celestijnenlaan 200F, 3001 Leuven, Belgium. E-mail: bert.sels@kuleuven.be

† Electronic supplementary information (ESI) available: Detailed experimental procedures; tables, graphs, figures and related analyses of the GC, GPC and NMR characterization of the lignin fractions. See DOI: 10.1039/d0sc04182c

Lignin is considered to be a structurally complex amorphous, aromatic polymer formed by radical polymerization of a set of oxygenated phenolic monomers in the plant cell wall. This polymerization – predominantly endwise – eventually produces a racemic polymer with different types of interphenolic linkages.[18–22] The β-O-4 ether inter-unit linkage is most abundant (40–80%). Other ether linkages originating from lignification are 4-O-5 and α-O-4, α-O-γ, and α-O-α, the latter three ether linkages always occurring in combination with a more resilient C–C inter-unit bond in the native lignin.[5,19] The most common C–C inter-unit structures are phenylcoumaran (β-5, α-O-4), resinol (β-β, 2x α-O-γ), dibenzodioxocin (5-5, β-O-4, α-O-4) and spirodienone (β-1, α-O-α).[19]

In commercial biorefining processes, like the pulp and paper industry, the C–O linkages are broken in harsh acidic or alkaline conditions, leaving reactive lignin-derived intermediates prone to irreversible C–C condensation. This results in recalcitrant, high molecular weight lignin products,[2,4,5,23] thus hampering the exploitation of lignin as a platform towards high value chemical products. Avoiding this condensation is of pivotal importance in novel biorefinery schemes.[24] In this respect, *lignin-first* approaches are currently under development, focusing primarily on the valorisation of lignin.[24–27] One

particular *lignin-first* refining technology, Reductive Catalytic Fractionation (RCF), has emerged notably in recent years.[24,28]

RCF targets a maximum carbon efficiency, by focusing primarily on lignin extraction, leaving most of the carbohydrates unaltered, mainly as pulp. In this biorefinery process, lignin is solvolytically extracted from its lignocellulosic matrix and the inter-unit ether linkages are being broken, generating reactive phenolic intermediates, in which the side-chains are stabilized upon reduction chemistry, creating less reactive groups to avoid irreversible C–C condensation.[28–32] In a typical RCF process, biomass is contacted with a polar, protic solvent (*e.g.* MeOH,[4,29,32–41] EtOH/H$_2$O,[42–44] iPrOH/H$_2$O[45–47]), a heterogeneous redox catalyst (*e.g.* Pd/C,[34,35,42,48–50] Ru/C,[33,51] Ni on various supports[29,31,32,37,45,52]) and a hydrogen source at elevated temperatures (200–250 °C). Afterwards, a highly depolymerized lignin oil is obtained with phenolic monomers (in close to theoretical yield based on ether interlinkages, up to 60 wt%), dimers and short oligomers.[4,28,53]

In fact, the analysis of similar hydrogenolysis oils has been used to elucidate lignin's *in planta* structure since the 1940s.[54–56] Although RCF is now being developed as a biorefining strategy, its use as powerful tool for the structural analysis of native lignin is gradually revisited.[31,57–60] Current characterization efforts of the RCF lignin oil are mainly focusing on the quantification of the lignin derived monomers, as well as on the identification of some phenolic dimers.[31,33–35] However, the chemical structure of the RCF lignin oligomers, at least 40% of the lignin oil content, remains largely unexplored. Detailed knowledge of the different functionalities, inter-phenolic linkages, as well as the molecular weight–functionality relationship, is important with regard to the unravelling of the RCF chemistry and to the future valorisation of RCF lignin oligomers to end products and materials. For instance, for technical Kraft lignin oligomer fractions, it was recently proven that the molecular weight impacts the number of phenolics and inter-unit linkages present per lignin molecule, influencing the properties of the resulting epoxy thermoset.[61]

The structural understanding of close to native lignin such as Milled Wood Lignin (MWL) and Cellulolytic Enzyme Lignin (CEL) has been greatly advanced thanks to the development and application of ^{1}H–^{13}C 2D heteronuclear single quantum coherence spectroscopy (HSQC) NMR.[62] This powerful technique enables qualification and semi-quantification of most structural inter-unit linkages in *in planta* lignin. In analogy, recent use of this 2D HSQC NMR on technical lignin (*e.g.* Kraft or Organosolv) is gradually improving the understanding of their molecular structure,[18,23,63–66] especially in a combinatorial approach together with sequential separation steps[67] and/or model compound studies.[66,68] For example, Bruijnincx and Lancefield *et al.* successfully applied this strategy to analyse Kraft lignin.[66] They showed the conversion of native C–C lignin linkages to Kraft analogue structures, and reported the assignment of up to 45% of the Kraft lignin structure.

Few 2D HSQC NMR studies reveal the effective cleavage of native C–O inter-unit linkages in *lignin-first* lignin oil.[30,33,34] Despite these studies, there is only little information available about the fate of the native inter-unit C–C linkages after RCF

processing. Encouraged by the recent results on technical (Kraft) lignin, this study aims to elucidate all main lignin inter-unit linkages in the lignin oil after the RCF processing of pine wood. Hereto, a variety of analytical techniques (2D HSQC NMR, GC-FID, GC-MS, ^{31}P-NMR and GPC) were used both on crude lignin oil and liquid–liquid extracted fractions thereof, leading to the assignment of more than 80% of structural units in the RCF lignin oil.

Results and discussion

In this study, pine wood was processed under benchmark RCF conditions at the 2 L scale. Pine wood, a common feedstock in lignocellulose biorefineries, was chosen because it is rich in guaiacyl units, entailing a higher, less complicated dimer and oligomer content after RCF processing, which is advantageous for this study. Therefore, 150 g of pine sawdust, 15 g of Pd/C (5 wt% Pd) and 800 mL methanol were added to a 2 L Parr batch reactor. The mixture was pressurized with hydrogen (30 bar at room temperature), stirred at 600 rpm and heated to 235 °C for a reaction time of 3 h. After cooling, filtration and DCM–water extraction; a stable, low molecular weight lignin oil (M_w 664 g mol^{-1}, F_{oil}) was obtained, representing 49 wt% of the Klason lignin content. Effective depolymerization is evidenced by the high content (34 wt%) of phenolic monomers in the resulting oil, corresponding to 16.7 wt% of phenolic monomers relative to the Klason lignin content. Within this monomer fraction, a high selectivity of 84% to 4-propanolguaiacol is observed (Fig. 1A, F_{oil}), which is consistent with literature.[34,35] Other monomers such as 4-propylguaiacol and 4-(3-methoxypropyl)guaiacol are also observed in lower concentration.

Furthermore, the RCF lignin's GPC profile shows a low molecular weight oil (Fig. 2, F_{oil}). In spite of the low molecular weight, its composition is heterogeneous containing a large
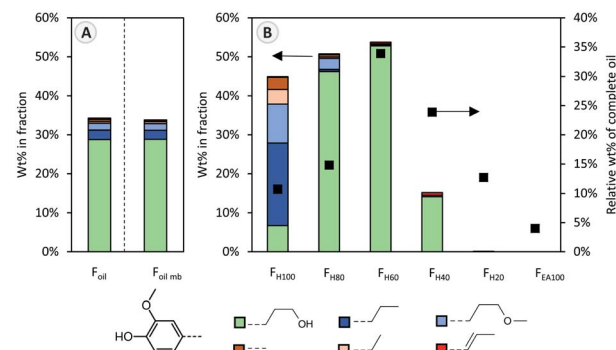

Fig. 1 Guaiacyl-monomer content (coloured bars), determined by GC analysis. Different colours represent different guaiacyl monomer types, characterized by different functional groups as shown in the legend. (A) Monomer content as weight percentage relative to the weight of the original oil (F_{oil}) and the monomeric mass balance ($F_{oil\ mb}$) which is constructed by multiplying the monomer content in each fraction (B) by its corresponding weight percentage. (B) Monomer content as weight percentage in the different fractions (F_x), as well as the weight percentage of each fraction relative to the crude oil (F_{oil}). More detailed information is available in Table S3.†
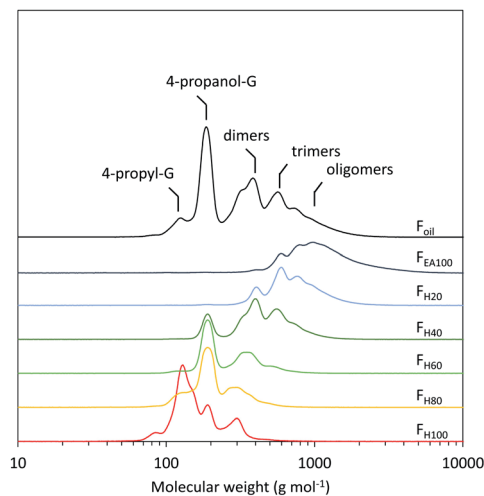
Fig. 2 GPC profiles of the obtained RCF oil (F_{oil}) and the six fractions (F_{H100}–F_{EA100}).

variety of phenolic dimers and oligomers, which complicates molecular structure analysis. Given this compositional complexity, the pine RCF lignin oil was first fractionated using a sequential solvent fractionation with a binary solvent mixture of heptane and ethyl acetate before further analysis. The mixture's polarity was sequentially altered by systematically increasing the ethyl acetate fraction by 20 volume% and decreasing the heptane fraction by 20 volume% (Fig. S1, Table S1, see ESI† for additional information). This sequential binary solvent fractionation resulted in six different fractions: F_{H100} (100 vol% heptane/0 vol% ethyl acetate), F_{H80} (80 vol% heptane/ 20 vol% ethyl acetate), and analogously F_{H60}, F_{H40}, F_{H20} and F_{EA100}. The obtained fractions were used for the subsequent analyses.

GC analysis

The sequential fractionation resulted in the enrichment of monomers in the first three fractions (F_{H100}, F_{H80}, and F_{H60}), compared to the RCF oil (Fig. 1B). Phenolic monomers account for 45 wt% of the heptane soluble fraction (F_{H100}), containing primarily apolar monomers such as 4-propylguaiacol and 4-(3-methoxypropyl)guaiacol, whilst only 2.5% of 4-propanolguaiacol of the entire lignin oil is found in this fraction. Clearly, heptane is not a suitable solvent to extract and solubilize 4-propanolguaiacol from the lignin oil.

4-Propanolguaiacol is the main lignin compound in fractions F_{H80} and F_{H60} (approximately 50 wt% in both fractions), for which respectively 20% and 40% ethyl acetate in heptane was used as extraction solvent. Thus, a slight increase in the solvent mixture's polarity significantly enhances 4-propanolguaiacol's solubility. Fraction F_{H40} still contains a small fraction of monomers, whereas fraction F_{H20} and F_{EA100} are monomer-free. Notably, as measure of reliability, the accumulated calculated mass balance of the monomers over each individual fraction (Fig. 1A, $F_{oil\ mb}$) is nearly identical to that of the analysed crude RCF oil (F_{oil}).

In addition to monomers, also dimers can be studied by GC (preferably after derivatization). It has already been reported that almost all inter-unit ether linkages in RCF lignin dimers are cleaved during RCF processing, whereas the C–C inter-unit linkages are expected to remain intact.[31–33,50,54,69] Indeed, a handful of dimers linked with C–C linkages (β-5, β-1, β-β, 5-5) are observed in the RCF lignin oil (Scheme 1). However, variations in these β-5, β-1 and β-β RCF dimers exist by having different substitutions of the inter-unit linkage. For example, dimers linked with an ethyl bridge (β-5 and β-1) can be either unsubstituted or substituted by a hydroxymethyl substituent (Scheme 1). Variations in β-5 and 5-5 dimers are present by alteration of the aliphatic end-unit. These variations in the end-unit are similar to the observed alkyl chains in RCF monomers. Differences in the distribution of these dimers within the six fractions are illustrated in Fig. S4–S6.† Dimers with two phenolic OH-functionalities and no aliphatic OH-functionalities are found mainly in the most apolar fractions, F_{H100} and F_{H80}, whereas dimers with 1 or 2 additional aliphatic OH-functionalities, *i.e.* 3 or 4 OH's in total, are extracted selectively into the more polar solvents (Fig. S6†).

GPC analysis

The number average molecular weights (M_n) of the six fractions show a consistent increase between 168 and 1239 g mol^{-1} with increasing amounts of ethyl acetate in the binary extraction solvent mixture (Table 1). This effect can be attributed to the increasing polarity of the solvent, since higher molecular weight lignin fragments contain more OH functionalities per molecule, resulting in a higher polarity (Fig. S3†). Notably, the fraction with the highest molecular weight (F_{EA100}) is solely composed of oligomers, implying that all monomers and dimers can be removed through extraction (Fig. 2). Moreover, all fractions are more homogeneous regarding their molecular weight compared to the crude oil, as evidenced by the significantly lower dispersity indices, *viz.* between 1.19 and 1.37, compared to 1.57 for the original crude lignin oil (F_{oil}). Interestingly, as a measure of reliability, the mass balanced GPC profile, wherein the normalized GPC profile of each fraction is multiplied by their respective weight percentage, is almost identical to the GPC profile of the crude RCF oil (F_{oil}) (Fig. S2†).

Assignment of 2D HSQC NMR spectrum

In contrast to GC for monomers and (to a lesser extent) dimers, 2D HSQC is the technique *par excellence* for analysing the
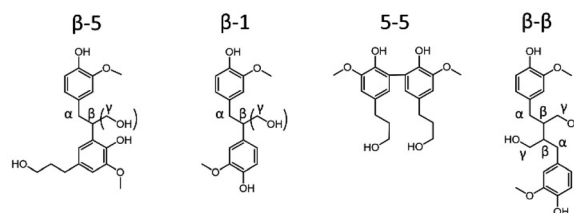
Scheme 1 Structure of main dimers in RCF lignin oil of pine wood.

Table 1 Mass distribution and molecular weight of the obtained RCF oil (F_{oil}) and the six fractions (F_{H100}-F_{EA100})

	F_{H100}	F_{H80}	F_{H60}	F_{H40}	F_{H20}	F_{EA100}	F_{oil}
Wt% in fraction	10.7	14.8	33.9	23.9	12.7	4.0	
M_n (g mol^{-1})	168	221	281	468	762	1239	420
M_w (g mol^{-1})	203	264	349	584	931	1771	667
DI	1.21	1.19	1.24	1.25	1.22	1.37	1.59

chemical structure of the entire lignin oil. However, many of the RCF C–C linkages, observed via GC-MS in dimers, are currently not assigned in the 2D HSQC NMR spectrum of RCF lignin. Based on literature research, we collected the chemical shifts of the ^1H and ^{13}C NMR spectra of the observed RCF inter-unit linkages in the dimers. However, these reported chemical shifts were measured in a variety of deuterated solvents (Table S4†). Since the NMR solvent can have a major impact on the chemical shifts, all inter-unit linkages have to be assigned in a single deuterated solvent.[70] To assign these chemical shifts, a high concentration of one specific inter-unit linkage is required. Remarkably, in some fractions the concentration of specific dimers and thus of certain inter-unit linkages is already relatively high (Fig. S5†). To enable the inevitable assignment of the chemical shifts, column chromatography was applied on selected fractions (F_{H80} and F_{H40}) to obtain fractions enriched in dimers with a β-5 γ-OH, β-1 γ-OH, β-β 2x γ-OH, β-5 ethyl, β-1 ethyl, β-β THF, and 5-5 inter-unit linkage, as evidenced by their GC and GC-MS (ESI Section 4†).

Subsequently, the 2D HSQC NMR spectra of these concentrated dimers were measured in DMSO-d$_6$. Comparison to literature data revealed small shifts of the chemical shifts due to the use of different NMR solvents (Table S4†). Afterwards, these spectra were compared to the 2D HSQC NMR spectra of the RCF lignin oil and the dimer-free F_{EA100} fraction, as a representative mixture of the RCF lignin oligomers (free of monomers and dimers) (Fig. S7–S14†). The 2D HSQC NMR spectra of the RCF lignin oil is presented in Fig. 3. Note that this approach results, to the best of our knowledge, in the first assignment of most, if not all, major RCF lignin structures in 2D HSQC NMR. Specifically, β-5 γ-OH, β-1 γ-OH, β-β 2x γ-OH, β-5 ethyl, β-1 ethyl, β-β THF, and 5-5 inter-unit linkages are assigned unambiguously now for the first time in the NMR spectrum of RCF lignin oil. We expected to assign β-5 propyl and β-1 propyl inter-unit linkages as well, but this was not possible due to their very low abundance and the inherent moderate detection limit of NMR. More importantly, the assignments (derived originally here from the dimer structures) are also applicable to the structural motifs in RCF oligomers, evidenced by the appearance of identical chemical shifts in the essentially mono- and dimer-free F_{EA100} fraction. This observation proves the structural similarity between dimers and oligomers, and thus indicates that they were subject of the same chemical transformations during RCF processing.

Furthermore, a low β-O-4 content is found in F_{EA100}, indicating their effective cleavage to aliphatic end-units. These end-units have the same aliphatic structure compared to those observed in the monomers (by GC). The assignment of these end-units in the monomers (such as 4-propanol, 4-propyl, 4-ethyl, 4-(3-methoxypropyl), 4-methyl and 4-propenol) has been described previously, but presence of these structures in the RCF lignin oligomers was not be unambiguously demonstrated until now.

Relative quantification via 2D HSQC NMR

Quantification of lignin inter-unit linkages has been frequently done via ^{13}C and 2D HSQC NMR.[71] However, such a quantitative assessment has never been performed on thoroughly characterized RCF lignin oil. 2D HSQC NMR is often the preferred NMR method due to a reduced measuring time and a superior resolution, effectively separating several overlapping cross-peaks in the ^{13}C NMR spectrum. Unfortunately, quantification by 2D HSQC NMR has its associated errors. Firstly, the inter-unit linkage quantification is typically expressed relative to a defined lignin cross peak, serving as the internal standard. This internal standard is often the methoxy region or a part of the aromatic region, enabling the inter-unit linkage quantification relative to the number of aromatic units, which are set to 100.[71] Here, we chose to use the aromatic G_2 area as internal standard, since it is the most common method for softwood lignin.[71] Since this integration method can introduce errors, they need verification, as is done here in this study. Other associated deviations of a 2D HSQC experiment are due to processing errors,[23] differences in amongst others T_1 and T_2 relaxation rates, and differences in coupling constants.[63,66,71,72] Techniques such as HSQC$_0$ have been developed to reduce some of these negative effects. Although promising, these methods are still not fully quantitative, as proven for some lignin dimers,[66] whilst the measuring time is increased fourfold. Therefore, we chose to measure the HSQC spectra with the standard pulse sequence (hsqcetgpsp.3), proven to have acceptable errors compared to the HSQC$_0$ experiment[66] and to minimise other possible deviations and time consumption. In order to reduce the processing deviations, the spectra were processed and integrated in triplicate. Furthermore, the quantitative character was validated by comparing the 2D HSQC results with quantitative ^{13}C NMR analysis, for which we have selected three of our fractions, viz. F_{oil}, F_{H80} and F_{EA100}, having varying molecular weight (Fig. S22, Table S7†). We found an underestimation of 3.4–7.6% for linkage abundance by using the G_2 signal as relative internal standard for the amount of aromatic units in RCF lignin. In addition, the G_2 integrals had only slightly higher values compared to that of the methoxy-region. Accordingly, at least for our case, the G_2 area is considered as a reliable internal standard. A next validation
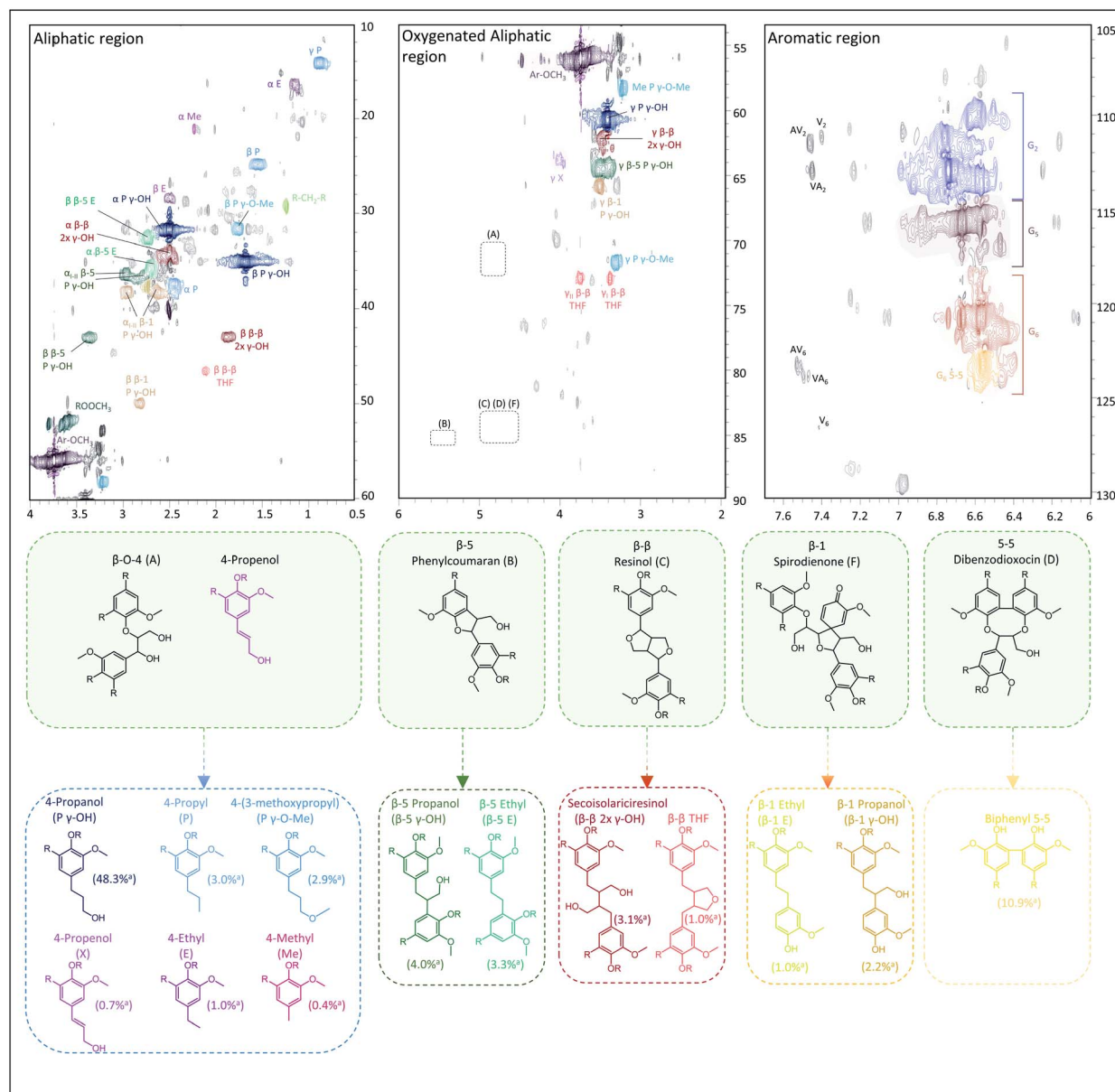
Fig. 3 Assignment of the 2D HSQC NMR spectrum of the crude pine RCF oil. The figure links the native inter-unit linkages (green background) with their corresponding RCF products during reductive catalytic fractionation of the wood (for conditions, see Experimental in ESI†). Fig. S7–S14 (provided in the ESI†) reveal all details to support the assignments. [a] Relative quantification vs. G_2 area, the spectra were processed in triplicate, more information can be found in Tables S5 and S6.†

effort compared the relative integrals of some well resolved shifts in the quantitative ^{13}C NMR spectra to their 2D HSQC NMR counterpart (Table S8†). No relative differences larger than 20%, most of them even smaller than 10%, were found in this assessment. Often the ^{13}C spectra gave slightly higher values, which can be partly attributed to signal overlapping. In general, the above results lead to the conclusion that the associated errors of a semi-quantitative evaluation of the RCF 2D HSQC spectrum are in an acceptable range.

The 2D HSQC analysis of the fractions shows clear fraction dependent trends of the structural motifs (Fig. 4 and S15–S19†), as expected from the GC analyses of the monomers and dimers.

These structural motifs (Fig. 3) can be divided into aliphatic end-units (see above) and inter-unit linkage groups, which are β-5, β-1, β-β, 5-5 and β-O-4. These two different groups and their relationship to the native lignin inter-unit linkages are discussed in the next section.

In the crude RCF oil (F_{oil}), 56.4% aliphatic end-units can be found relative to the amount of aromatics, originating from β-O-4, dibenzodioxocin, and 4-propenol motives in native lignin. Within this group, the 4-propanol end-units (P γ-OH) are most abundant with a selectivity of 85%. Remarkably, when compiling of the mass balance of all fractions ($F_{oil\ mb}$) a similar number of end-units (56.1%) is shown, but the selectivity to P γ-
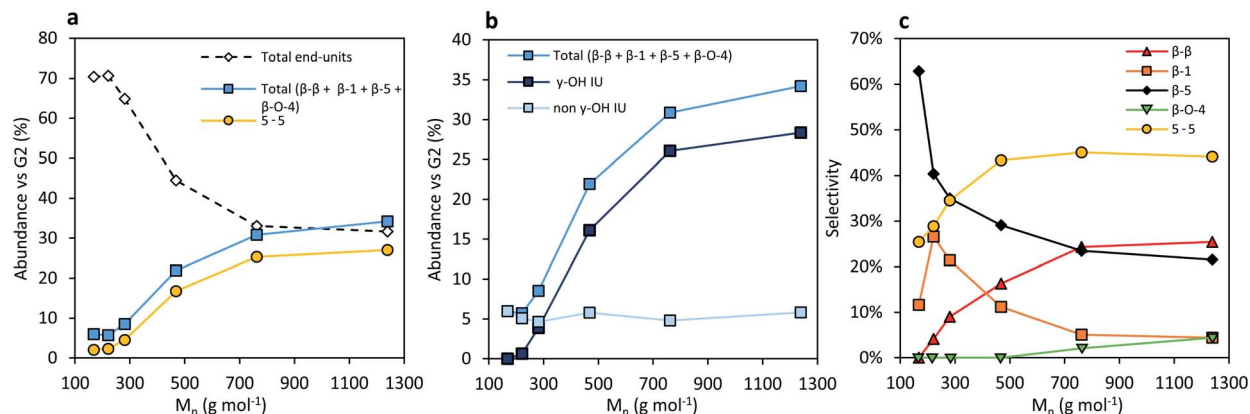
Fig. 4 Distribution of several inter-unit linkages and end-units in respect to the number average molecular weight (M_n) of the fractions. (a) Comparison of the linkage abundance of the total end-units, total sum of β-β, β-1, β-5 and β-O-4, and 5-5 as determined by 2D HSQC NMR relative to the G_2 area. (b) Comparison of the total β-β, β-1, β-5 and β-O-4 inter-unit (IU) linkages in each fraction to their γ-OH substituted and their non γ-OH substituted analogues. (c) Selectivities of β-β, β-1, β-5, β-O-4 and 5-5 inter-unit linkages.

OH is somewhat reduced to 79% (Table S6†). Possibly, this is due to T_2 relaxation effects, indicating a relatively higher amount of 4-propanol end-units in the smaller molecules.[66,73] A similar relaxation time dependent trend was observed by Bruijnincx et al. who studied the M_n dependence of stilbene-units.[66] An observable trend over all fractions is the steady decrease of aliphatic end-units with increasing molecular weight (Fig. 4a). In F_{H100} more 4-(3-methoxypropyl)guaiacol (P γ-O-Me) and 4-propyl (P) units are present compared to P γ-OH, in line with the GC results. In all other fractions, the selectivity to P γ-OH is dominant, and declines steadily with increasing molecular weight to a selectivity of 78% in F_{EA100} (Fig. S15†). The latter evidences selectivity differences of P γ-OH with increasing molecular weight. Furthermore, native β-O-4 linkages are only found in small amounts in the two fractions, viz. F_{H20} and F_{EA100} with the highest molecular weight, proving the effective cleavage of this ether linkage and conversion to end-units due to RCF processing.

The second group of molecular structures in the RCF lignin oil are the inter-unit linkages. In total, they account for 25.8% of the molecular signals, relative to the number of aromatics.

The first group of these inter-unit linkages are β-5 linkages. No native β-5 phenylcoumaran units were found in the crude RCF lignin oil. This inter-unit linkage is converted completely by hydrogenolysis to form β-5 γ-OH and β-5 (E) RCF analogues. The analysis shows 7.3% of these non-native β-5 units in the crude oil (F_{oil}) with a slightly higher selectivity to the γ-OH linkage (Fig. 3). More of these two β-5 inter-unit linkages can be found in the fractions with higher molecular weight in accordance with the higher phenolic content, and thus inter-unit linkages, per molecule with increasing MW. Interestingly, the selectivity to β-5 γ-OH units is low, viz. 0–30%, in the low molecular weight fractions and plateaus around 70–80% in the higher molecular weight fractions.

β-β linkages are the second group of major inter-unit linkages. Similarly to native β-5 linkages, no native β-β resinol structures were found in the RCF oil, suggesting their effective

complete conversion to their β-β 2x γ-OH and β-β THF RCF analogues under the RCF operational conditions. Although not the focus of this manuscript, their formation is directly related to the hydrogenolysis chemistry of Pd catalysis in presence of hydrogen. A total of 4.1% β-β units can be found in the crude oil (F_{oil}). The number of β-β linkages clearly increases with increasing molecular weight. Furthermore, a higher amount of γ-OH substitution is observed at the higher molecular weight fragments (Fig. S18†). These observations are in line with the aforementioned explanations for β-5 inter-unit linkages.

The third group are the β-1 inter-unit linkages, originating from the spirodienone units in native lignin. After RCF processing, this native inter-unit linkage is absent in the crude lignin oil, and converted to β-1 γ-OH and β-1 E. Around 3% of β-1 structural motifs can be found in the RCF oil, with a higher selectivity of 67% to its γ-OH analogue (Fig. S17†). A higher amount of γ-OH substitution is observed at the higher molecular weight fragments (Fig. S17†), similar to the observations of the β-β and β-5 inter-unit linkage. However, in contrast to these other inter-unit linkages, the number of β-1 motifs does not change with the molecular weight. This can be attributed to the condition that one of the phenolic units in the β-1 linkage always has to be a non-substituted, free phenolic unit, originating from the ketone of the spirodienone structure in native lignin. As a result, the relative chance of coupling a β-1 inter-unit linkage with another C–C linkage during the radical polymerization is lower compared to the other inter-unit linkages.[19] Consequently, their relative abundance in RCF oligomers is lower.

The last group of inter-unit linkages are biphenyl (5-5) units. They are known to be abundant in softwoods, and are originally present in the dibenzodioxocin structure. In this pine derived oil, the content of 5-5 units is 10.9%, in line with literature reports on structural analysis of the native lignin.[74,75] In line with the bonding strength,[18] these original 5-5 units thus survive RCF processing. Not surprisingly, its concentration profile in function of the molecular weight shows a similar increasing trend as the β-5 and β-β profile (Fig. 4a).

Given the 25.8% of assigned inter-unit linkages and 56.4% of assigned end-units, this results in a total assignment of over 82% of the 2D HSQC spectrum of this crude RCF oil (F_{oil}). In contrast, when no catalyst is used, only 26% of the 2D HSQC spectrum can be assigned (Table S11†). This clearly indicates the importance of the redox catalyst in steering the selectivity of this process. Besides, this value is also high in comparison to the recently reported 45% for technical Kraft lignin, even though many of its inter-unit linkages and end-units were assigned.[66] A large portion of the unaccounted assignments in Kraft lignin, as well as in the catalyst-free organosolv process, is due to the C–C re-condensation reactions, occurring after β-O-4 cleavage, since a large gap between native β-O-4 linkages and Kraft-derived structures exist.[66] This is in stark contrast to the stabilized RCF lignin. Given this high value of structural assignment for crude RCF lignin oil, general structural rationalisation may now be possible, with regard to the original lignin structure and tuning of chemical (*e.g.* reactivity) and physical (*e.g.* rheology) properties. The latter remains difficult for cases where less than half of the structures are known, *e.g.* in the case of Kraft lignin.

A proof of concept of the possibility to alter the functionality of the RCF lignin is demonstrated by comparing the selectivities of the inter-unit linkages of RCF performed at 195 °C and 235 °C (Fig. S21†). Clearly, the selectivity to OH-substituted inter-unit linkages is higher at the lower temperature. Further research with regard to the selectivity control at different reaction conditions is needed and work in progress.

Correlation of the several inter-unit linkages assigned with the molecular weight shows interesting trends (Fig. 4). In the higher molecular weight fractions a considerably higher amount of γ-hydroxyl functionality in the inter-unit linkages of β-β, β-5 and β-1 is observed (Fig. 4b), compared to the amount of inter-unit linkages without the γ-OH functionality that remains equal with the molecular weight. At least partially, this can be attributed to a solubility difference, as is clearly shown in the dimer analysis. Oligomers with hydroxyl functionalities in their inter-unit linkage are more polar, impeding the extraction in less polar solvents. However, chemical reactivity differences of the γ-OH in high molecular weight RCF lignin fragments cannot be excluded. We speculate that the latter is due to (pore) diffusional or (surface) coordinative difficulties with the catalyst, due to the more demanding steric effects of the high molecular weight molecules.

Another important observation is that the amount of 5-5 inter-unit linkages is considerably higher relative to the other inter-unit linkages in fractions with higher molecular weight (Fig. 4c). The rationalization of this observation can be found in the native structure of lignin and their boundary conditions of inter-unit linkages. On the one hand, the phenols of a 5-5 unit after RCF will always be non-etherified phenolic due to the dibenzodioxocin structure, whilst it has two aliphatic chains. Both aliphatic chains can be C–C linked with a β-5, β-β or β-1 linkage to form a trimer. On the other hand, both aliphatic chains have to be linked with a β-O-4 linkage or contain an end-unit to form a dimer. As a result, the chance of its incorporation

in a RCF lignin oligomer is relatively higher compared to other inter-unit linkages.

^{31}P-NMR

Besides identification and understanding of formation of the structural motifs in crude RCF lignin, the hydroxyl content is another important parameter considering its valorisation potential, as it strongly determines the chemical reactivity and physical properties. A frequently applied method to determine the OH-content is phosphorylation of lignin with 2-chloro-4,4,5,5-tetramethyl-1,3,2-dioxaphospholane followed by ^{31}P-NMR spectroscopy. Table S9† summarizes the measurements of the different fractions.

A total OH content of 9.16 mmol OH g^{-1} was found in the complete crude lignin oil (F_{oil}), of which the phenolic OH content was found 4.78 mmol OH g^{-1} and the aliphatic OH content 4.29 mmol OH g^{-1}. All fractions show a high hydroxylic content above 4 mmol OH g^{-1} (Fig. 5) except for the pure hexane F_{H100} fraction. Here, a distinctly lower amount of aliphatic OH can be found (1.14 mmol OH g^{-1}). This is in line with the expectation given the low amount of extracted 4-propanol end-units during the apolar extraction step with pure heptane, as previously discussed. Furthermore, the amount of phenolics per gram oil in F_{H100} is lower compared to the other fractions, which is most likely due to the presence of significant amounts of extractives in this fraction. This is supported by a low observable amount of monomers and dimers (in wt%) and by a higher amount of methylated carboxylic groups and R-CH$_2$-R signals that are not lignin-derived, relative to the other fractions (Fig. S20†).

A general trend is the increase of 5-substituted guaiacyl units with higher molecular weight, while the unsubstituted phenolic units decrease (Fig. S24†). This result is as expected, since the observed amount of β-5 and 5-5 substitution determined by ^{31}P-NMR and 2D HSQC NMR correlates well, confirming the validity of both complementary analyses (Fig. S24†).

Moreover, the amount of phenolic OH decreases slightly in the higher molecular weight fractions, which can be attributed
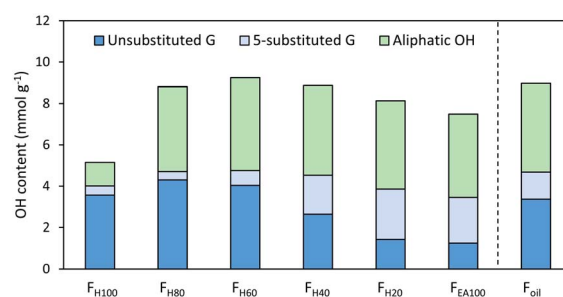
Fig. 5 Hydroxyl group content of all fractions and the RCF oil (F_{oil}) quantified by ^{31}P-NMR and expressed as mmol per gram oil. Measurements were performed in triplicate. Unsubstituted G are guaiacyl units without substitution at position 5 of the aromatic ring, 5-substituted G is the sum of β-5, 5-5 and 4-O-5 substitution on the aromatic G ring. More detailed information on ^{31}P-NMR can be found in Table S9.†
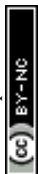
to the presence of small amounts of unreacted β-O-4 and 4-O-5 and units (Fig. S26†). After RCF processing, these 4-O-5 units are present in 2.7% relative to the number of phenols in the crude lignin oil. This number clearly increases with increasing molecular weight to 9.2% in F_{EA100} (Fig. S25†). These 4-O-5 inter-unit linkages are not included in the ^1H–^{13}C HSQC NMR analysis, since there was no unambiguously assignment of them in the aromatic area of the NMR spectrum.

Structural relation to native lignin

Hydrogenolysis of lignocellulose has been used to produce lignin-derived products valuable to gain more structural insight in the structure of native lignin. For instance, by studying the obtained monomers and dimers, particularly in old literature with notice of a recent revival, successful genetic lignin engineering can be proven.[31,33,54,57,69] Furthermore, the existence of a relationship between the β-O-4 content of lignin and the amount of monomers obtained after the catalytic hydrogenolysis in the RCF step has been frequently postulated,[5,26,33,72,76] obtaining similar results as by applying thioacidolysis.[31,58] Given the extended structural insight and toolbox generated in this work, we revisited the catalytic hydrogenolysis (under RCF conditions) as an analytical tool by comparing the molecular structures found in Milled Wood Lignin (MWL) and the molecular structures in crude RCF lignin oil. The results of this comparison are illustrated in Table 2.

MWL was obtained from the same pine as used to produce the RCF lignin oil, representing 21 wt% of the Klason lignin content. Since the degree of delignification between MWL (21 wt%) and RCF (49 wt%) differs considerably, care has to be taken to compare the lignins, since the composition of the extracted lignin might differ.[77] Since RCF operates at a higher delignification, the resulting lignin oil is thus more representative for the entire, native lignin fraction. The structural motifs present in MWL that can be expected to result in RCF end-units, viz. β-O-4, 4-propenal, 4-propenol, 4-propanol and dibenzodioxocin, amount to 58.4%. In comparison, the amount of aliphatic end-units present in the RCF oil equals 56.7%, suggesting a near-quantitative conversion of these structural native lignin units to their RCF analogues. This is in accordance with negligible C–C condensation during RCF involving the lignin

side chains. A similar comparison can be constructed for β-5 and β-β units, which have less than 16% relative mass balance variations between MWL and RCF oil. At first sight, the dibenzodioxocin mass balance seems less consistent with the RCF results. However, 2 aromatic guaiacyl units are connected in 1 dibenzodioxocin structure, giving a theoretical total of 10.4 guaiacyl units with a 5-5 inter-unit linkage from MWL. This number is similar to the analysed amounts after the RCF wood processing step (10.9%). Despite the differences in delignification between RCF lignin and MWL, the above observations clearly highlight the applicability of RCF as an analytical tool for structural analysis of lignin by using now the extended toolbox of assignments disclosed herein. The analysis now goes significantly beyond the study of only monomers and dimers, as initiated by a.o. Hibbert, Pepper and Sakakibara,[56] as it enables also a representative study of (almost all) the lignin inter-unit linkages of the entire lignin oil, hereby extracting indispensable molecular structural information, not shown as complete as before.

Conclusion

Structural details of lignin derived intermediate products, produced in lignin-first biorefineries, is imperative to achieve their successful and efficient valorisation in end user applications. In this contribution a thorough structural elucidation of RCF lignin oil was conducted by combining solvent fractionation and a variety of chromatographic (GC, GC-MS, GPC and chromatographic separations) and spectroscopic (various one and two D NMR) analysis techniques. This led to an unprecedented understanding, in particular of the before largely unknown molecular structure of the oligomeric RCF lignin components. The study delivers, to the best of our knowledge, the first assignment of novel (unnatural) β-5 γ-OH, β-1 γ-OH, β-β 2x γ-OH, β-5 ethyl, β-1 ethyl, β-β THF and 5-5 inter-unit linkages in the 2D HSQC NMR spectrum of the RCF lignin oil. We demonstrate for a typical RCF softwood lignin (pine) that more than 80% of its structural linkages can now be assigned unambiguously. Furthermore, a comprehensive analysis of the different RCF lignin fractions revealed that almost no C–C condensation occurs and indicated the existence of a fraction-dependent linkage abundance. Based on these results, more dedicated research into the differences in selectivity of the inter-unit linkages and the role of catalysis is needed. Such further research could also help to determine the quantity of specific oligomers, effectively helping to close the mass balance.

A comparison of MWL and RCF lignin showed that most of the MWL inter-unit linkages, representing original native lignin, are converted to a select set of RCF analogues, limiting the structural complexity of the RCF lignin product stream. To improve the insights gained from this study, comparable efforts must be made on RCF lignins derived from different feedstock and process conditions (e.g., temperature, catalyst type, solvent…). Likely, other distributions and few other inter-unit linkages will be found. Furthermore, novel 2D HSQC NMR methods can be developed, explored and used to further reduce the quantitative error on the analysis of RCF lignin. Overall, this

Table 2 Integration results of 2D HSQC NMR of MWL lignin, the crude RCF oil and the mass balanced RCF oil

	MWL[a,b,d]	RCF oil[a,c,d]	RCF oil$_{mb}$[a,d]
β-O-4 (A)/end-units	58.4	56.7	56.4
β-5 (B)	8.7	7.3	7.5
β-β (C)	3.9	4.1	4.3
5-5 (D)	5.2	10.9	10.4
β-1 (F)	1.3	3.2	2.9

[a] Detailed results of specific structural units are shown in Table S12. [b] The structural MWL units are shown in Fig. S28. [c] The structural RCF units are shown in Fig. 3. [d] The semi-quantification is relative to the G_2 area of the corresponding spectra and expressed as per 100 G_2 units.

study will ultimately advance future lignin valorisation efforts and will enable the search for tailored lignin properties through tailoring of RCF catalysts, besides optimization of the operational process conditions.

Conflicts of interest

There are no conflicts to declare.

Acknowledgements

Notes and references

1 A. J. Ragauskas, J. T. Beckham, M. J. Biddy, R. Chandra, F. Chen, M. F. Davis, B. H. Davison, R. A. Dixon, P. Gilna, M. Keller, P. Langan, A. K. Naskar, J. N. Saddler, T. J. Tschaplinski, G. A. Tuskan and C. E. Wyman, *Science*, 2014, **344**, 1246843.

2 J. Zakzeski, P. C. A. Bruijnincx, A. L. Jongerius and B. M. Weckhuysen, *Chem. Rev.*, 2010, **110**, 3552–3599.

3 C. Li, X. Zhao, A. Wang, G. W. Huber and T. Zhang, *Chem. Rev.*, 2015, **115**, 11559–11624.

4 Z. Sun, B. Fridrich, A. de Santi, S. Elangovan and K. Barta, *Chem. Rev.*, 2018, **118**, 614–678.

5 W. Schutyser, T. Renders, S. den Bosch, S.-F. Koelewijn, G. T. Beckham and B. F. Sels, *Chem. Soc. Rev.*, 2018, **47**, 852–908.

6 A. Deneyer, E. Peeters, T. Renders, S. Van den Bosch, N. Van Oeckel, T. Ennaert, T. Szarvas, T. I. Korányi, M. Dusselier and B. F. Sels, *Nat. Energy*, 2018, **3**, 969–977.

7 Y. Liao, S.-F. Koelewijn, G. Van den Bossche, J. Van Aelst, S. Van den Bosch, T. Renders, K. Navare, T. Nicolaï, K. Van Aelst, M. Maesen, H. Matsushima, J. M. Thevelein, K. Van Acker, B. Lagrain, D. Verboekend and B. F. Sels, *Science*, 2020, **367**, 1385–1390.

8 X. Ouyang, X. Huang, M. D. Boot and E. J. M. Hensen, *ChemSusChem*, 2020, **13**, 1705–1709.

9 S. Song, J. Zhang, G. Gözaydın and N. Yan, *Angew. Chem., Int. Ed.*, 2019, **58**, 4934–4937.

10 C. Xu, E. Paone, D. Rodríguez-Padrón, R. Luque and F. Mauriello, *Chem. Soc. Rev.*, 2020, **49**, 4273–4306.

11 M. Balat, *Energy Convers. Manage.*, 2011, **52**, 858–875.

12 M. J. Climent, A. Corma and S. Iborra, *Green Chem.*, 2014, **16**, 516–547.

13 D. M. Alonso, J. Q. Bond and J. A. Dumesic, *Green Chem.*, 2010, **12**, 1493–1513.

14 F. G. Calvo-Flores, J. A. Dobado, J. Isac-Garcia and F. J. Martin-Martinez, *Lignin and Lignans as Renewable Raw Materials*, 2015, pp. 247–288.

15 F. H. Isikgor and C. R. Becer, *Polym. Chem.*, 2015, **6**, 4497–4559.

16 I. van Zandvoort, E. J. Koers, M. Weingarth, P. C. A. Bruijnincx, M. Baldus and B. M. Weckhuysen, *Green Chem.*, 2015, **17**, 4383–4392.

17 G. Tsilomelekis, M. J. Orella, Z. Lin, Z. Cheng, W. Zheng, V. Nikolakis and D. G. Vlachos, *Green Chem.*, 2016, **18**, 1983–1993.

18 R. Rinaldi, R. Jastrzebski, M. T. Clough, J. Ralph, M. Kennema, P. C. A. Bruijnincx and B. M. Weckhuysen, *Angew. Chem., Int. Ed.*, 2016, **55**, 8164–8215.

19 J. Ralph, C. Lapierre and W. Boerjan, *Curr. Opin. Biotechnol.*, 2019, **56**, 240–249.

20 R. Vanholme, B. Demedts, K. Morreel, J. Ralph and W. Boerjan, *Plant Physiol.*, 2010, **153**, 895–905.

21 R. Vanholme, B. De Meester, J. Ralph and W. Boerjan, *Curr. Opin. Biotechnol.*, 2019, **56**, 230–239.

22 W. Boerjan, J. Ralph and M. Baucher, *Annu. Rev. Plant Biol.*, 2003, **54**, 519–546.

23 S. Constant, H. L. J. Wienk, A. E. Frissen, P. de Peinder, R. Boelens, D. S. van Es, R. J. H. Grisel, B. M. Weckhuysen, W. J. J. Huijgen, R. J. A. Gosselink and P. C. A. Bruijnincx, *Green Chem.*, 2016, **18**, 2651–2665.

24 T. Renders, S. den Bosch, S.-F. Koelewijn, W. Schutyser and B. F. Sels, *Energy Environ. Sci.*, 2017, **10**, 1551–1557.

25 A. De Santi, M. V. Galkin, C. W. Lahive, P. J. Deuss and K. Barta, *ChemSusChem*, 2020, **13**, 4468–4477.

26 W. Lan, M. T. Amiri, C. M. Hunston and J. S. Luterbacher, *Angew. Chem., Int. Ed.*, 2018, **57**, 1356–1360.

27 D. S. Zijlstra, C. W. Lahive, C. A. Analbers, M. B. Figueirêdo, Z. Wang, C. S. Lancefield and P. J. Deuss, *ACS Sustainable Chem. Eng.*, 2020, **8**, 5119–5131.

28 T. Renders, G. Van den Bossche, T. Vangeel, K. Van Aelst and B. Sels, *Curr. Opin. Biotechnol.*, 2019, **56**, 193–201.

29 E. M. Anderson, M. L. Stone, M. J. Hülsey, G. T. Beckham and Y. Román-Leshkov, *ACS Sustainable Chem. Eng.*, 2018, **6**, 7951–7959.

30 E. M. Anderson, M. L. Stone, R. Katahira, M. Reed, G. T. Beckham and Y. Román-Leshkov, *Joule*, 2017, **1**, 613–622.

31 E. M. Anderson, M. L. Stone, R. Katahira, M. Reed, W. Muchero, K. J. Ramirez, G. T. Beckham and Y. Román-Leshkov, *Nat. Commun.*, 2019, **10**, 2033.

32 S. den Bosch, T. Renders, S. Kennis, S.-F. Koelewijn, G. den Bossche, T. Vangeel, A. Deneyer, D. Depuydt, C. M. Courtin, J. M. Thevelein, W. Schutyser and B. F. Sels, *Green Chem.*, 2017, **19**, 3313–3326.

33 S. den Bosch, W. Schutyser, R. Vanholme, T. Driessen, S.-F. Koelewijn, T. Renders, B. De Meester, W. J. J. Huijgen, W. Dehaen, C. M. Courtin, B. Lagrain, W. Boerjan and B. F. Sels, *Energy Environ. Sci.*, 2015, **8**, 1748–1763.

34 S. den Bosch, W. Schutyser, S.-F. Koelewijn, T. Renders, C. M. Courtin and B. F. Sels, *Chem. Commun.*, 2015, **51**, 13158–13161.

35 W. Schutyser, S. den Bosch, T. Renders, T. De Boe, S.-F. Koelewijn, A. Dewaele, T. Ennaert, O. Verkinderen, B. Goderis, C. M. Courtin and B. F. Sels, *Green Chem.*, 2015, **17**, 5035–5045.

36 T. Parsell, S. Yohe, J. Degenstein, T. Jarrell, I. Klein, E. Gencer, B. Hewetson, M. Hurt, J. I. Kim, H. Choudhari, B. Saha, R. Meilan, N. Mosier, F. Ribeiro, W. N. Delgass, C. Chapple, H. I. Kenttämaa, R. Agrawal and M. M. Abu-Omar, *Green Chem.*, 2015, **17**, 1492–1499.

37 I. Klein, B. Saha and M. M. Abu-Omar, *Catal. Sci. Technol.*, 2015, **5**, 3242–3245.

38 E. M. Anderson, R. Katahira, M. Reed, M. G. Resch, E. M. Karp, G. T. Beckham and Y. Román-Leshkov, *ACS Sustainable Chem. Eng.*, 2016, **4**, 6940–6950.

39 T. Vangeel, T. Renders, K. Van Aelst, E. Cooreman, S. den Bosch, G. den Bossche, S.-F. Koelewijn, C. M. Courtin and B. F. Sels, *Green Chem.*, 2019, **21**, 5841–5851.

40 Z. Sun, G. Bottari, A. Afanasenko, M. C. A. Stuart, P. J. Deuss, B. Fridrich and K. Barta, *Nat. Catal.*, 2018, **1**, 82–92.

41 S. Li, W. Li, Q. Zhang, R. Shu, H. Wang, H. Xin and L. Ma, *RSC Adv.*, 2018, **8**, 1361–1370.

42 T. Renders, S. Van den Bosch, T. Vangeel, T. Ennaert, S.-F. Koelewijn, G. Van den Bossche, C. M. Courtin, W. Schutyser and B. F. Sels, *ACS Sustainable Chem. Eng.*, 2016, **4**, 6894–6904.

43 M. V. Galkin and J. S. M. Samec, *ChemSusChem*, 2014, **7**, 2154–2158.

44 M. V. Galkin, A. T. Smit, E. Subbotina, K. A. Artemenko, J. Bergquist, W. J. J. Huijgen and J. S. M. Samec, *ChemSusChem*, 2016, **9**, 3280–3287.

45 P. Ferrini and R. Rinaldi, *Angew. Chem., Int. Ed.*, 2014, **53**, 8634–8639.

46 I. Graça, R. T. Woodward, M. Kennema and R. Rinaldi, *ACS Sustainable Chem. Eng.*, 2018, **6**, 13408–13419.

47 C. Chesi, I. B. D. de Castro, M. T. Clough, P. Ferrini and R. Rinaldi, *ChemCatChem*, 2016, **8**, 2079–2088.

48 X. Huang, O. M. Morales Gonzalez, J. Zhu, T. I. Korányi, M. D. Boot and E. J. M. Hensen, *Green Chem.*, 2017, **19**, 175–187.

49 X. Huang, J. Zhu, T. I. Korányi, M. D. Boot and E. J. M. Hensen, *ChemSusChem*, 2016, **9**, 3262–3267.

50 T. Renders, W. Schutyser, S. Van den Bosch, S.-F. Koelewijn, T. Vangeel, C. M. Courtin and B. F. Sels, *ACS Catal.*, 2016, **6**, 2055–2066.

51 T. Renders, E. Cooreman, S. den Bosch, W. Schutyser, S.-F. Koelewijn, T. Vangeel, A. Deneyer, G. den Bossche, C. M. Courtin and B. F. Sels, *Green Chem.*, 2018, **20**, 4607–4619.

52 W. Mu, X. Wang, Q. Xue, B. Jiang, T. Zhang and M. Miao, *Food Res. Int.*, 2012, **47**, 364–367.

53 M. V. Galkin and J. S. M. Samec, *ChemSusChem*, 2016, **9**, 1544–1558.

54 A. Sakakibara, *Hydrogenolysis*, ed. S. Y. Lin and C. W. Dence, Springer Berlin Heidelberg, Berlin, Heidelberg, 1992, pp. 350–368.

55 F. G. Calvo-Flores, J. A. Dobado, J. Isac-Garcia and F. J. Martin-Martinez, in *Lignin and Lignans as Renewable Raw Materials*, John Wiley & Sons, Ltd, 2015, pp. 189–246.

56 A. Sakakibara, in *Methods in Lignin Chemistry*, ed. S. Y. Lin and C. W. Dence, Springer Berlin Heidelberg, Berlin, Heidelberg, 1992, pp. 350–368.

57 P. Oyarce, B. De Meester, F. Fonseca, L. de Vries, G. Goeminne, A. Pallidis, R. De Rycke, Y. Tsuji, Y. Li, S. Van den Bosch, B. Sels, J. Ralph, R. Vanholme and W. Boerjan, *Nat. Plants*, 2019, **5**, 225–237.

58 K. M. Torr, D. J. van de Pas, B. Nanayakkara and I. D. Suckling, *Holzforschung*, 2014, **68**, 151.

59 M. L. Stone, E. M. Anderson, K. M. Meek, M. Reed, R. Katahira, F. Chen, R. A. Dixon, G. T. Beckham and Y. Román-Leshkov, *ACS Sustainable Chem. Eng.*, 2018, **6**, 11211–11218.

60 Y. Li, L. Shuai, H. Kim, A. H. Motagamwala, J. K. Mobley, F. Yue, Y. Tobimatsu, D. Havkin-Frenkel, F. Chen, R. A. Dixon, J. S. Luterbacher, J. A. Dumesic and J. Ralph, *Sci. Adv.*, 2018, **4**, eaau2968.

61 C. Gioia, G. Lo Re, M. Lawoko and L. Berglund, *J. Am. Chem. Soc.*, 2018, **140**, 4054–4061.

62 C. Crestini, F. Melone, M. Sette and R. Saladino, *Biomacromolecules*, 2011, **12**, 3928–3935.

63 C. Crestini, H. Lange, M. Sette and D. S. Argyropoulos, *Green Chem.*, 2017, **19**, 4104–4121.

64 C. Nitsos, R. Stoklosa, A. Karnaouri, D. Vörös, H. Lange, D. Hodge, C. Crestini, U. Rova and P. Christakopoulos, *ACS Sustainable Chem. Eng.*, 2016, **4**, 5181–5193.

65 H. Yang, C. G. Yoo, X. Meng, Y. Pu, W. Muchero, G. A. Tuskan, T. J. Tschaplinski, A. J. Ragauskas and L. Yao, *Bioresour. Technol.*, 2020, **295**, 122240.

66 C. S. Lancefield, H. L. J. Wienk, R. Boelens, B. M. Weckhuysen and P. C. A. Bruijnincx, *Chem. Sci.*, 2018, **9**, 6348–6360.

67 H. Lange, P. Schiffels, M. Sette, O. Sevastyanova and C. Crestini, *ACS Sustainable Chem. Eng.*, 2016, **4**, 5136–5151.

68 C. W. Lahive, P. J. Deuss, C. S. Lancefield, Z. Sun, D. B. Cordes, C. M. Young, F. Tran, A. M. Z. Slawin, J. G. de Vries, P. C. J. Kamer, N. J. Westwood and K. Barta, *J. Am. Chem. Soc.*, 2016, **138**, 8900–8911.

69 K. Sudo, D. J. Mullord and J. M. Pepper, *Can. J. Chem.*, 1981, **59**, 1028–1031.

70 G. R. Fulmer, A. J. M. Miller, N. H. Sherden, H. E. Gottlieb, A. Nudelman, B. M. Stoltz, J. E. Bercaw and K. I. Goldberg, *Organometallics*, 2010, **29**, 2176–2179.

71 J.-L. Wen, S.-L. Sun, B.-L. Xue and R.-C. Sun, *Materials*, 2013, **6**, 359–391.

72 M. Talebi Amiri, S. Bertella, Y. M. Questell-Santiago and J. S. Luterbacher, *Chem. Sci.*, 2019, **10**, 8135–8142.

73 H. Okamura, H. Nishimura, T. Nagata, T. Kigawa, T. Watanabe and M. Katahira, *Sci. Rep.*, 2016, **6**, 21742.

74 P. Azadi, O. R. Inderwildi, R. Farnood and D. A. King, *Renewable Sustainable Energy Rev.*, 2013, **21**, 506–523.

75 F. G. Calvo-Flores, J. A. Dobado, J. Isac-Garcia and F. J. Martin-Martinez, in *Lignin and Lignans as Renewable Raw Materials*, John Wiley & Sons, Ltd, 2015, pp. 9–48.

76 T. Phongpreecha, N. C. Hool, R. J. Stoklosa, A. S. Klett, C. E. Foster, A. Bhalla, D. Holmes, M. C. Thies and D. B. Hodge, *Green Chem.*, 2017, **19**, 5131–5143.

77 H. Lange, P. Giannì and C. Crestini, in *Lignin Valorization: Emerging Approaches*, The Royal Society of Chemistry, 2018, pp. 413–476.